

Received: 2017.12.12
Accepted: 2018.09.07
Published: 2019.01.28

Matrix Metalloproteases-Mediated Cleavage on β -Dystroglycan May Play a Key Role in the Blood-Brain Barrier After Intracerebral Hemorrhage in Rats

Authors' Contribution:
Study Design A
Data Collection B
Statistical Analysis C
Data Interpretation D
Manuscript Preparation E
Literature Search F
Funds Collection G

BEG 1 **Xin Zhang**
BG 2 **Yunhe Gu**
C 1 **Peitong Li**
D 1 **Anqi Jiang**
F 3 **Xiaomeng Sheng**
F 4 **Xin Jin**
C 1 **Yue Shi**
A 1 **Guozhong Li**

1 Department of Neurology, The First Affiliated Hospital of Harbin Medical University, Harbin, Heilongjiang, P.R. China
2 Department of Pathology, The First Affiliated Hospital of Harbin Medical University, Harbin, Heilongjiang, P.R. China
3 Department of Neurology, Harbin Fourth Hospital, Harbin, Heilongjiang, P.R. China
4 Department of Neurology, Jixi People's Hospital, Jixi, Heilongjiang, P.R. China

Corresponding Author: Guozhong Li, e-mail: lgzhyd1962@163.com

Source of support: This study was supported by grants from the Postdoctoral Scientific Research Developmental Foundation of Heilongjiang Province (No. LBH-Q15106) and the Research Foundation of Health and Family Planning Commission of Heilongjiang Province (No. 2014-273)

Background: It is well documented that the Blood-Brain barrier (BBB) can be damaged by matrix metalloproteases (MMPs) after intracerebral hemorrhage (ICH), but little is known about the mechanism of this effect.

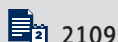
Material/Methods: We established an ICH model in rats by injecting collagenase VII into the striatum. Afterwards, intraperitoneal injection of these rats with 40 mg/kg GM6001 (a MMPs inhibitor). The effects of GM6001 on ICH were investigated by neurological severity score, brain water content, Evans blue staining, hematoxylin-eosin staining, immunohistochemical staining, and Western blot assays.

Results: We demonstrated that the neurological damage caused by ICH was relieved at 5 and 7 days following administration of GM6001. The impaired BBB induced by ICH was improved in response to GM6001 treatment at around 3 days, as evidenced by alleviated cerebral edema, decreased Evans blue extravasation, and a reduction in inflammatory cellular infiltration. Mechanism analysis revealed that ICH induced the generation of β -dystroglycan cleavage, which could be suppressed by GM6001 treatment. Furthermore, we found that recombinant MMP2 and MMP9 triggered the cleavage of β -dystroglycan *in vitro*, and this action could be inhibited by GM6001 administration.

Conclusions: Taken together, our results suggest that MMPs-mediated cleavage on β -dystroglycan may play an important role in BBB after ICH.

MeSH Keywords: **Blood-Brain Barrier • Cerebral Hemorrhage • Dystroglycans • Matrix Metalloproteinases**

Full-text PDF: <https://www.medscimonit.com/abstract/index/idArt/908500>



2109



5



36



Background

Intracerebral hemorrhage (ICH) accounts for about 15% of all strokes, with 1-month mortality rates of 50% in patients after ICH [1]. Previous studies have demonstrated that the Blood–Brain barrier (BBB) integrity was disrupted in brain damage after ICH, leading to neurological deficits, inflammatory responses, and cerebral edema [2,3]. The BBB consists of endothelial cells (ECs), pericytes, astrocytes, neurons, and the extracellular matrix (ECM) [4]. The interaction between receptors on ECs/astrocytes and ligands on ECM elicits diverse molecular signals that probably regulate BBB functions [5].

Dystroglycan (DG), one of the main ECM receptors, consists of a highly glycosylated extracellular alpha subunit (α -DG) and a transmembrane beta subunit (β -DG) [6]. Previous studies have demonstrated that DG plays a critical role in a variety of pathophysiological processes, such as cancers, muscle diseases, and embryonic development [7–10]. Hawkins et al. suggested DG may play a vital role in BBB integrity and aggravate brain edema after oxygen/glucose deprivation (OGD) [11]. β -DG was found to be degraded by matrix metalloproteases (MMPs), a family of zinc endopeptidases, which can disrupt the link between the ECM and cell membrane [12,13]. Moreover, previous reports have shown that the BBB can be damaged by MMPs after ICH [14,15]. However, the mechanisms of MMPs during BBB breakdown after ICH are not entirely clear.

In the present study, the ICH model was induced in rats by injection of collagenase VII into the striatum. Then, the effect of GM6001 (a MMPs inhibitor) on neurological damage, the BBB, and the expression of β -DG in these rats was determined.

Material and Methods

Animals

Male Wistar rats, weighing 250 to 300 g, were obtained from the Animal Center of Harbin Medical University (Harbin, China). The animals were raised in a room maintained at $22\pm 1^\circ\text{C}$ with 12-h light/dark cycles, and food and water were available *ad libitum*. This study was approved by the Institutional Animal Care and Use Committee of Harbin Medical University and performed according to the National Institutes of Health Guidelines for the Care and Use of Laboratory Animals.

ICH model establishment and treatment

The rat ICH model was established based on the previous literature [16]. In brief, rats were anesthetized with pentobarbital sodium by intraperitoneal injection, and fixed in a brain stereotaxic apparatus (Jiangwan, Shanghai, China). ICH was

induced by stereotaxic injection of 0.5 U collagenase VII (diluted in 1.0 μl saline; Sigma-Aldrich, Milwaukee, WI, USA) into the striatum (location: 0.2 mm anterior, 3.0 mm right lateral, and 6 mm ventral to the bregma). Sham-operated rats were injected with 1.0 μl saline. Then, the burr hole was sealed with bone wax and the wound was sutured.

A total of 405 rats were randomly assigned to 3 groups: Sham ($n=139$), ICH group (133), and ICH + GM6001 group (133). After establishment of the ICH model, rats in the ICH + GM6001 group received MMPs blocker GM6001 (Chemicon International, Temecula, CA, USA) by intraperitoneal injection per day after ICH. GM6001 was dissolved in 0.2% DMSO and administered at the dose of 40 mg/kg body weight.

Behavioral testing

Neurocognitive function was evaluated using the neurological severity score (NSS) [17], including motor, sensory, reflex, and balance tests, with a total score of 18 points (normal score, 0; maximal deficit score, 18), with higher scores indicating more severe injury. The NSS test was performed in rats ($n=7/\text{group}$) at days 1, 2, 3, 5, and 7 after the operation by an investigator who was blinded to the experimental groups.

Brain water content

Brain water content was evaluated in rats ($n=7/\text{group}$) at days 1, 2, 3, 5, and 7 after the operation. Briefly, the brains isolated from rats were divided into the ipsilateral and contralateral hemispheres, and the pons and olfactory bulb were removed. The ipsilateral hemisphere tissue was weighed to obtain wet weight (ww) and then baked at 100°C for 24 h to obtain dry weight (dw). The water content was calculated as: $(\text{ww}-\text{dw})/\text{ww}\times 100$.

BBB permeability to Evans blue

BBB integrity was measured in rats ($n=7/\text{group}$) at days 1, 2, 3, 5, and 7 after the operation using Evans blue dye (Sigma-Aldrich) as described previously [18]. Briefly, Evans blue dye solution (2% in saline, 4 ml/kg) was intravenously infused over 1 min and allowed to circulate for 2 h prior to sacrifice. Then, the rats were anesthetized and transcardially perfused with 250 ml saline until colorless perfusion fluid was obtained. Thereafter, the brains were weighed after removing the olfactory bulbs and cerebellum, and placed in formamide (1 ml/100 mg; Sigma-Aldrich) for 48 h at 37°C . The absorbance of the supernatant solution was measured by a spectrophotometer at 620 nm (Thermo Fisher Scientific, Waltham, MA, USA). The tissue content of Evans blue was quantified from an Evans blue standard curve and normalized to tissue weight ($\mu\text{g}/\text{g}$).

Hematoxylin-eosin (HE) staining

HE staining was employed to detect the infiltrated inflammatory cells in brain tissues of rats ($n=7/\text{group}$). In brief, brain tissues were collected and prepared as 5- μm -thick paraffin-embedded sections. After dewaxing in xylene and rehydrating in a series of graded alcohols, the sections were dyed with hematoxylin (Solarbio, Beijing, China) for 5 min, differentiated using 1% hydrochloric acid alcohol solution for 3 s, and stained with eosin (Sangon, Shanghai, China) for 3 min. Then, the sections were dehydrated and mounted with neutral balsam. The images were captured using an optical microscope (Olympus, Tokyo, Japan).

Immunohistochemical staining (IHC)

The expression levels of myeloperoxidase (MPO) and ionized calcium-binding adaptor molecule 1 (IBA-1) in brain tissues were determined by IHC. Briefly, paraffin-embedded sections were deparaffinized, rehydrated, and subjected to antigen retrieval. Endogenous peroxidase was eliminated with 3% H_2O_2 for 15 min. Then, sections were blocked with goat serum for 15 min and incubated with primary antibodies against MPO (1: 200; Boster, Wuhan, China) and IBA-1 (1: 2000; Abcam, Cambridge, MA, UK) overnight at 4°C. After incubation with second antibody and HRP-conjugated avidin, the protein was visualized using DAB with hematoxylin counterstain. The stained sections were analyzed under a microscope (Olympus).

Hippocampal extracts and treatment

The hippocampi isolated from sham-operated rats ($n=6$) were homogenized in homogenization buffer according to previous research [19]. After centrifugation, the supernatant was collected and the protein concentration was determined by use of a BCA protein quantitative kit (Beyotime Institute of Biotechnology, Haimen, China). Then, the 100- μg sample was mixed with 100 ng of recombinant MMP2, or 100 ng of recombinant MMP9, or both, or with 100 ng of recombinant MMP2 + 0.5 nM GM6001, or with 100 ng of recombinant MMP9 + 0.2 nM GM6001, for 1 h at 37°C. Thereafter, Western blot analysis was used to evaluate the expression of β -DG.

Western blot analysis

Proteins were extracted from perihematomal tissues of rats by use of RIPA lysis buffer (Beyotime Institute of Biotechnology) after surgery at 3 day ($n=7$ each). The protein concentration was measured by the BCA method. The samples were separated by 10% SDS-PAGE, transferred to polyvinylidene fluoride membranes (Millipore, Billerica, MA, USA) and blocked in 5% nonfat milk in tris-buffered saline containing 0.1% tween 20 for 2 h. The membranes were incubated with the primary

antibodies against β -DG (1: 500; Proteintech, Wuhan, China) and β -tubulin (1: 500; Proteintech) at 4°C overnight, followed by incubation with horseradish peroxidase-conjugated goat anti-rabbit secondary antibody for 45 min at 37°C. The immunoblots were visualized with an enhanced chemiluminescence (ECL) detection kit (Beyotime Institute of Biotechnology). Images were semiquantitatively analyzed using Image J 4.0 (Media Cybernetics, Silver Spring, MD, USA). The intensity of the bands was normalized to β -tubulin.

Statistical analysis

The difference between 2 independent groups was analyzed with Mann-Whitney U test or the *t* test. Data are expressed as the mean \pm standard deviation (SD). All calculations were performed using GraphPad Prism 7.0 software (GraphPad, La Jolla, CA, USA), and $P<0.05$ was considered statistically significant.

Results

Inhibition of MMPs alleviated neurological deficits of rats with ICH

We first established a model of ICH in rats, and then studied the effect of GM6001 on neurological damage through the NSS test. As shown in Figure 1, ICH led to significant functional deficits in rats, which was relieved by GM6001 treatment at 5 and 7 days.

Inhibition of MMPs restrained cerebral edema, Evans blue extravasation, and inflammatory cellular infiltration in rats with ICH

Subsequently, we explored the effects of GM6001 on BBB in rats with ICH. As shown in Figure 2A, administration of GM6001 alleviated the cerebral edema in the ipsilateral brain caused by ICH at 3 and 5 days. The BBB permeability to Evans blue was significantly enhanced after ICH, and was inhibited by GM6001 treatment at day 3 (Figure 2B). The inflammatory cellular infiltration caused by ICH was clearly inhibited at 3 and 5 days following GM6001 administration through HE staining (Figure 3A). Moreover, the results of IHC showed that the expression levels of MPO and IBA-1, the marker of neutrophils and microglia, respectively, were significantly increased in the ICH model at around days 3 and 5, and were inhibited after GM6001 treatment (Figure 3B, 3C).

Inhibition of MMPs restrained the generation of β -DG cleavage

Considering the close relationship between MMPs and β -DG, we investigated the effect of GM6001 on the expression of β -DG

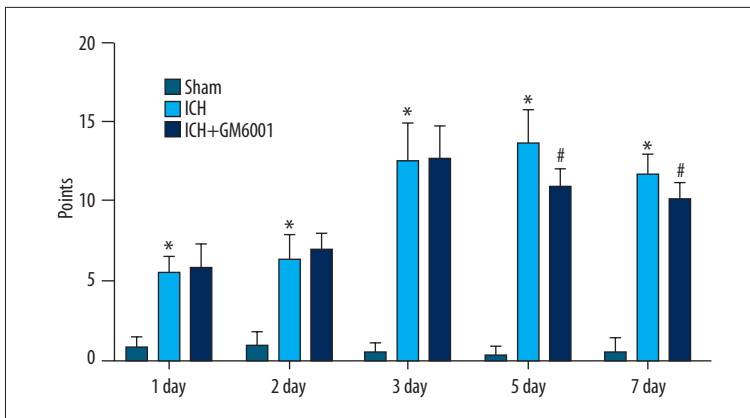


Figure 1. The neurological state of each group of rats at days 1, 2, 3, 5, and 7 was evaluated by NSS test. Data shown as mean \pm SD (n=7/group). * Compared to Sham, $P<0.0001$; # compared to ICH group, $P<0.0001$.

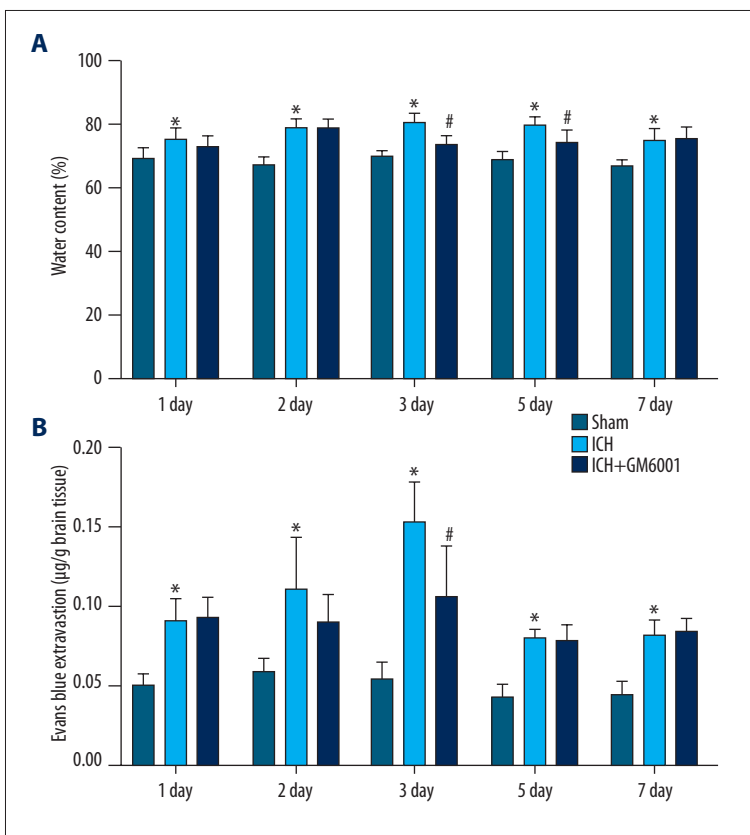


Figure 2. (A) The brain water content and (B) BBB permeability to Evans blue of each group of rats at days 1, 2, 3, 5, and 7 were determined. Data shown as mean \pm SD (n=7/group). * Compared to Sham, $P<0.05$; # compared to ICH group, $P<0.05$.

at 3 day in rats after ICH. As shown in Figure 4, Western blot assay revealed that the cleavage of β -dystroglycan at 31 kD was increased in rats subjected to ICH, and was inhibited following GM6001 treatment.

The regulation of β -dystroglycan cleavage by MMPs was further confirmed *in vitro*. As shown in Figure 5, we demonstrated that when the brain protein extracted from sham rats (n=6) was incubated with recombinant protein MMP2, MMP9, or both, the cleavage of β -dystroglycan at 31 kD was increased, and this action was inhibited by treatment with GM6001, indicating that MMPs mediated the cleavage of β -dystroglycan.

Discussion

In this study, we demonstrated that the integrity of the BBB was destroyed, presenting nerve dysfunction, brain edema, increased BBB permeability, and inflammatory cellular infiltration after ICH in rats, and the MMPs inhibitor alleviated these damages. All our results were in line with previous reports [20,21]. More importantly, we found that the MMPs was involved in the abnormal generation of β -DG cleavage in ICH.

The BBB plays an important role in maintaining homeostasis of the central nervous system [22]. It has been reported that

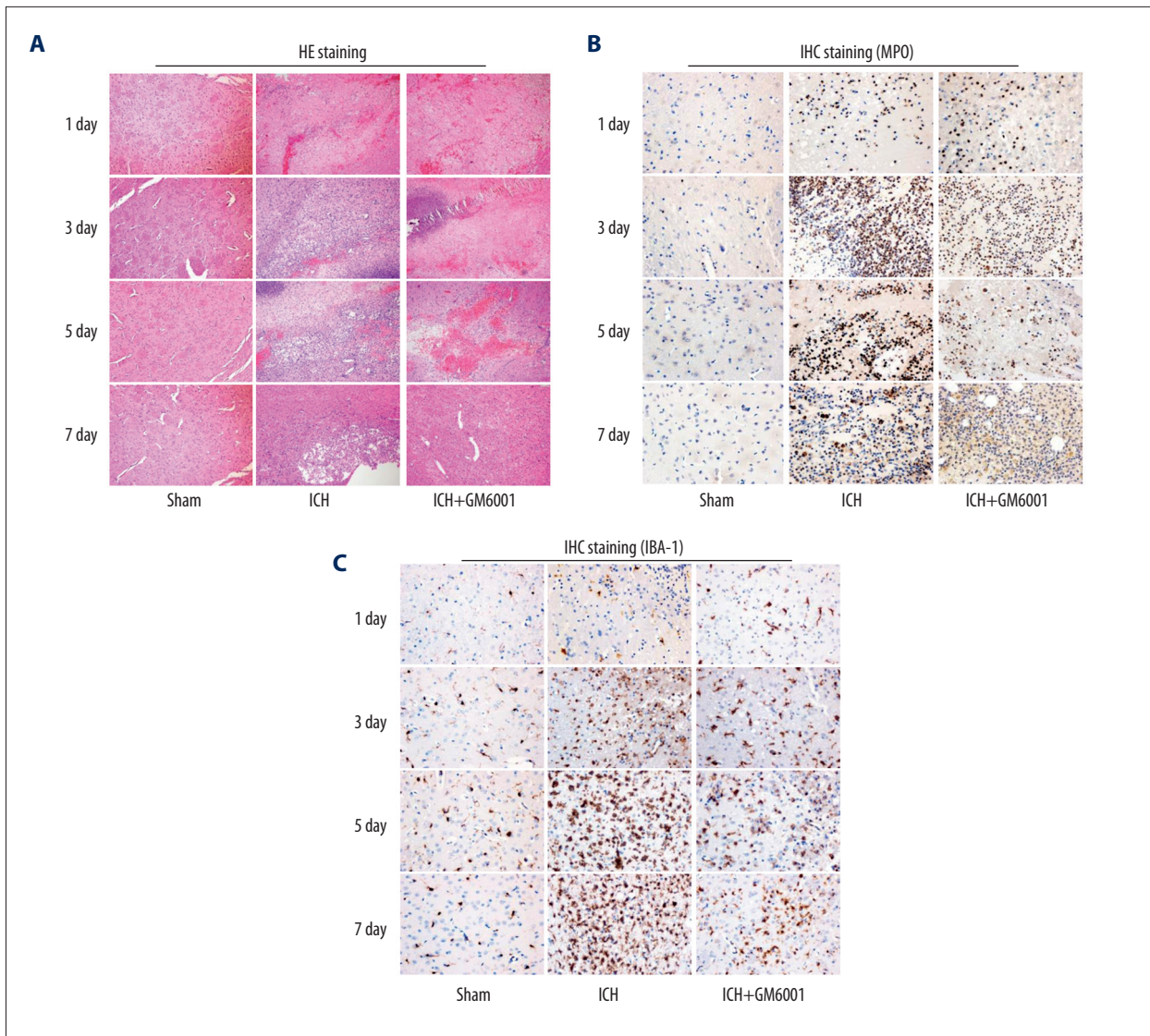


Figure 3. (A) Brain tissue inflammatory cell infiltration was examined by HE staining (100 \times). The expression levels of (B) MPO and (C) IBA-1 were determined by IHC (400 \times).

the BBB was disrupted after ICH both in human and in animal models [2,23,24]. MMPs are an important group of proteolytic enzymes that are capable of degrading the basement membrane and certain cell membrane proteins. The role of MMPs in hemorrhagic stroke appears to be critical for hematoma and brain edema, which are understood as secondary brain injuries and can have a considerable clinical impact [25,26].

Experimental models and clinical studies provided increasing evidence that inflammatory reactions are early triggered by hematoma components, enhance the damage within the hemorrhagic brain, and influence the prognosis. The inflammatory response begins immediately after the ICH onset. Hematoma components initiate inflammatory signaling via activation of microglia, which subsequently favors peripheral inflammatory

infiltration. Neutrophils are the earliest leukocytes recruited from peripheral blood into the brain; they are found in and around the hematoma as early as 4 h after collagenase-induced ICH, and peak at 2 to 3 days. The neutrophil-induced neurotoxicity is related to a multitude of pathways, including the upregulation of MMPs [27,28]. Clinically, these events are reflected by the early rise of peripheral neutrophils, which has been demonstrated to reliably predict stroke outcome, risk of early neurological deterioration, and functional recovery [29–31]. In the present study we demonstrated that microglia and neutrophils were significantly increased in the ICH model and were inhibited by GM6001 treatment.

The close combination of DG and ECM is probably required to maintain normal structure and function of the BBB [32].

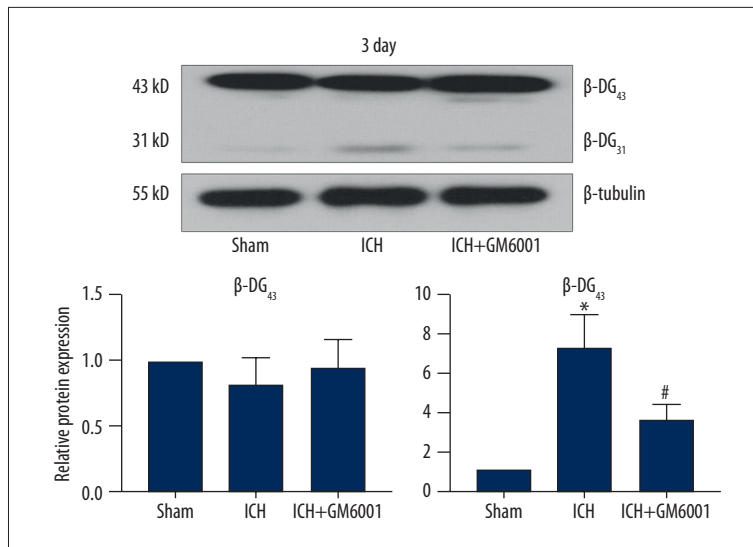


Figure 4. The expression of β -DG was examined through Western blot analysis in different groups of rats at day 3. The bands were quantified by densitometric analysis and normalized to β -tubulin expression. Data shown as mean \pm SD (n=7/group). * Compared to Sham, $P<0.01$; # compared to ICH group, $P<0.01$.

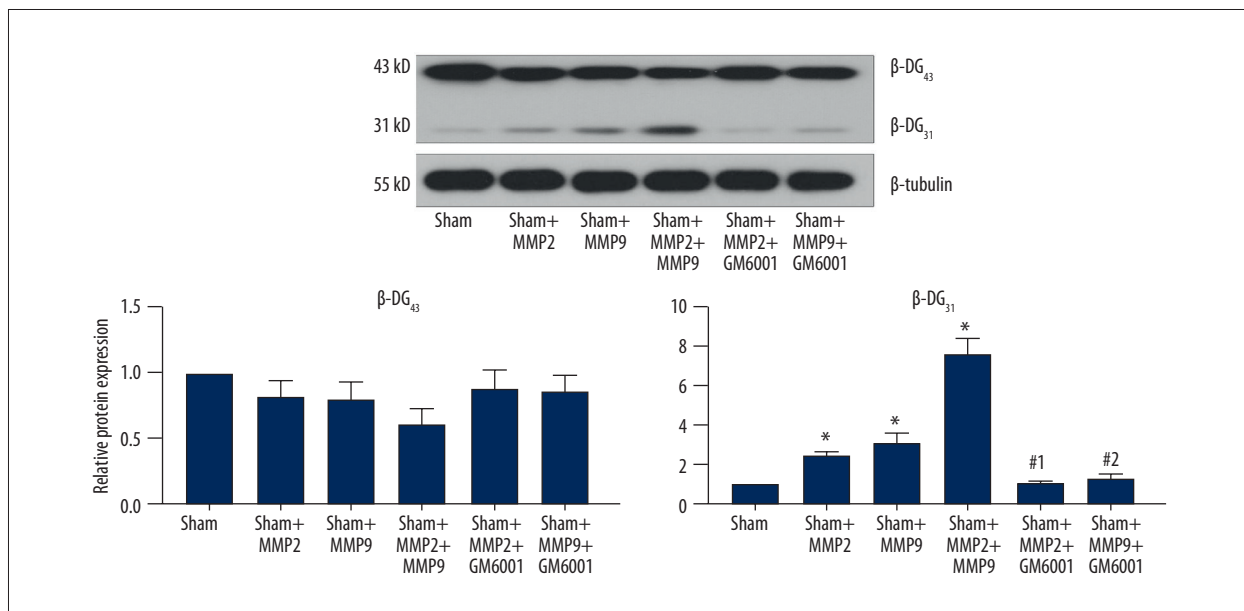


Figure 5. The level of β -DG was assessed by Western blot analysis in different groups. The bands were quantified by densitometric analysis and normalized to β -tubulin expression. Data shown as mean \pm SD (n=6/group). * Compared to Sham, $P<0.01$; #1 compared to Sham + MMP2 group, $P<0.01$; #2 compared to Sham + MMP9 group, $P<0.01$.

The expression of DG is closely related to the polarity of aquaporin-4, which is a water channel protein contributing to brain water homeostasis [33,34]. Moreover, under various pathological conditions, such as sarcoglycan-deficient skeletal muscle and acute cerebral ischemia [35,36], β -DG is abnormally cleaved, and this kind of anomalous expression is always associated with MMPs. Based on the above findings, we further studied the effect of MMP inhibitor (GM6001) on β -DG expression in rats with ICH. Our results showed that GM6001 administration decreased the expression of β -DG cleavage at 31 kD caused by ICH. Moreover, recombinant MMP2 and MMP9 triggered the generation of β -DG cleavage *in vitro*, which was inhibited by

GM6001 treatment, confirming the regulation of β -DG cleavage by MMPs in a rat ICH model.

Conclusions

Here, we showed that (i) MMPs was involved in BBB disruption after ICH, and (ii) MMPs was involved in β -DG abnormal splitting after ICH, which might be a cause of BBB disruption and aggravated cerebral injury.

Conflict of interest

None.

References:

- Sacco S, Marini C, Toni D et al: Incidence and 10-year survival of intracerebral hemorrhage in a population-based registry. *Stroke*, 2009; 40: 394–99
- Keep RF, Xiang J, Ennis SR et al: Blood–Brain barrier function in intracerebral hemorrhage. *Acta Neurochir Suppl*, 2008; 105: 73–77
- Kathirvelu B, Carmichael ST: Intracerebral hemorrhage in mouse models: Therapeutic interventions and functional recovery. *Metab Brain Dis*, 2015; 30: 449–59
- Khatri R, McKinney AM, Swenson B, Janardhan V: Blood–Brain barrier, reperfusion injury, and hemorrhagic transformation in acute ischemic stroke. *Neurology*, 2012; 79: 552–57
- Almutairi MM, Gong C, Xu YG et al: Factors controlling permeability of the Blood–Brain barrier. *Cell Mol Life Sci*, 2016; 73: 57–77
- Noell S, Wolburg-Buchholz K, Mack AF et al: Evidence for a role of dystroglycan regulating the membrane architecture of astroglial endfeet. *Eur J Neurosci*, 2011; 33: 2179–86
- Sgambato A, Di Salvatore MA, De Paola B et al: Analysis of dystroglycan regulation and functions in mouse mammary epithelial cells and implications for mammary tumorigenesis. *J Cell Physiol*, 2006; 207: 520–29
- Kanagawa M: [Dystroglycan glycosylation and muscular dystrophy]. *Seikagaku*, 2014; 86: 452–63 [in Japanese]
- Barresi R, Campbell KP: Dystroglycan: From biosynthesis to pathogenesis of human disease. *J Cell Sci*, 2006; 119: 199–207
- Bello V, Moreau N, Sirour C et al: The dystroglycan: Nestled in an adhesome during embryonic development. *Dev Biol*, 2015; 401: 132–42
- Hawkins BT, Gu YH, Izawa Y, Del Zoppo GJ: Disruption of dystroglycan-laminin interactions modulates water uptake by astrocytes. *Brain Res*, 2013; 1503: 89–96
- Li H, Mittal A, Makonchuk DY, Bhatnagar S, Kumar A: Matrix metalloproteinase-9 inhibition ameliorates pathogenesis and improves skeletal muscle regeneration in muscular dystrophy. *Hum Mol Genet*, 2009; 18: 2584–98
- Shang ZJ, Ethunandan M, Gorecki DC, Brennan PA: Aberrant expression of beta-dystroglycan may be due to processing by matrix metalloproteinases-2 and -9 in oral squamous cell carcinoma. *Oral Oncol*, 2008; 44: 1139–46
- Min H, Hong J, Cho IH et al: TLR2-induced astrocyte MMP9 activation compromises the blood brain barrier and exacerbates intracerebral hemorrhage in animal models. *Mol Brain*, 2015; 8: 23
- Chang JJ, Emanuel BA, Mack WJ et al: Matrix metalloproteinase-9: Dual role and temporal profile in intracerebral hemorrhage. *J Stroke Cerebrovasc Dis*, 2014; 23: 2498–505
- Sun H, Tang Y, Guan X et al: Effects of selective hypothermia on Blood–Brain barrier integrity and tight junction protein expression levels after intracerebral hemorrhage in rats. *Biol Chem*, 2013; 394: 1317–24
- Wang Y, Deng Y, Zhou GQ: SDF-1 α /CXCR4-mediated migration of systemically transplanted bone marrow stromal cells towards ischemic brain lesion in a rat model. *Brain Res*, 2008; 1195: 104–12
- Lee K, Lee BJ, Bu Y: Protective effects of dihydrocaffeic acid, a coffee component metabolite, on a focal cerebral ischemia rat model. *Molecules*, 2015; 20: 11930–40
- Michaluk P, Kolodziej L, Mioduszevska B et al: Beta-dystroglycan as a target for MMP-9, in response to enhanced neuronal activity. *J Biol Chem*, 2007; 282: 16036–41
- Wang J, Tsirka SE: Neuroprotection by inhibition of matrix metalloproteinases in a mouse model of intracerebral haemorrhage. *Brain*, 2005; 128: 1622–33
- Kawakita K, Kawai N, Kuroda Y et al: Expression of matrix metalloproteinase-9 in thrombin-induced brain edema formation in rats. *J Stroke Cerebrovasc Dis*, 2006; 15: 88–95
- Jalali S, Huang Y, Dumont DJ, Hynynen K: Focused ultrasound-mediated bbb disruption is associated with an increase in activation of AKT: Experimental study in rats. *BMC Neurol*, 2010; 10: 114
- Wagner KR, Xi G, Hua Y et al: Ultra-early clot aspiration after lysis with tissue plasminogen activator in a porcine model of intracerebral hemorrhage: Edema reduction and Blood–Brain barrier protection. *J Neurosurg*, 1999; 90: 491–98
- Rosenberg GA, Estrada E, Kelley RO, Kornfeld M: Bacterial collagenase disrupts extracellular matrix and opens Blood–Brain barrier in rat. *Neurosci Lett*, 1993; 160: 117–19
- Florczyk-Rzepka M, Grond-Ginsbach C, Montaner J, Steiner T: Matrix metalloproteinases in human spontaneous intracerebral hemorrhage: An update. *Cerebrovasc Dis*, 2012; 34: 249–62
- Chen YC, Ho WM, Lee YS et al: Polymorphisms in the promoters of the MMP-2 and TIMP-2 genes are associated with spontaneous deep intracerebral hemorrhage in the Taiwan population. *PLoS One*, 2015; 10: e0142482
- Zhou Y, Wang Y, Wang J et al: Inflammation in intracerebral hemorrhage: From mechanisms to clinical translation. *Prog Neurobiol*, 2014; 115: 25–44
- Chen S, Yang Q, Chen G, Zhang JH: An update on inflammation in the acute phase of intracerebral hemorrhage. *Transl Stroke Res*, 2015; 6: 4–8
- Lattanzi S, Cagnetti C, Rinaldi C et al: Neutrophil-to-lymphocyte ratio improves outcome prediction of acute intracerebral hemorrhage. *J Neurol Sci*, 2018; 387: 98–102
- Lattanzi S, Cagnetti C, Provinciali L, Silvestrini M: Neutrophil-to-lymphocyte ratio and neurological deterioration following acute cerebral hemorrhage. *Oncotarget*, 2017; 8: 57489–94
- Lattanzi S, Cagnetti C, Provinciali L, Silvestrini M: Neutrophil-to-lymphocyte ratio predicts the outcome of acute intracerebral hemorrhage. *Stroke*, 2016; 47: 1654–57
- Zaccaria ML, Di Tommaso F, Brancaccio A et al: Dystroglycan distribution in adult mouse brain: A light and electron microscopy study. *Neuroscience*, 2001; 104: 311–24
- Qiu GP, Xu J, Zhuo F et al: Loss of AQP4 polarized localization with loss of beta-dystroglycan immunoreactivity may induce brain edema following intracerebral hemorrhage. *Neurosci Lett*, 2015; 588: 42–48
- Tham DK, Joshi B, Moukhles H: Aquaporin-4 cell-surface expression and turnover are regulated by dystroglycan, dynamin, and the extracellular matrix in astrocytes. *PLoS One*, 2016; 11: e0165439
- Yan W, Zhao X, Chen H et al: beta-Dystroglycan cleavage by matrix metalloproteinase-2/-9 disturbs aquaporin-4 polarization and influences brain edema in acute cerebral ischemia. *Neuroscience*, 2016; 326: 141–57
- Fukai Y, Ohsawa Y, Ohtsubo H et al: Cleavage of beta-dystroglycan occurs in sarcolemma-deficient skeletal muscle without MMP-2 and MMP-9. *Biochem Biophys Res Commun*, 2017; 492: 199–205